was made. Full-matrix least-squares refinement minimized the function $[\sum w(|F_o| - |F_c|)^2/\sum w|F_o|^2]^{1/2}$, where $w = 1/[\sum(F_o)^2 + (pF_o)^2]$.

4 and 5 were crystallized in a triclinic system. The positions of Fe atoms were located by the direct method (4) and the Patterson method (5). Subsequent difference Fourier maps revealed the positions of all atoms. All non-hydrogen atoms were refined with anisotropic thermal parameters and all hydrogen atoms with isotropic thermal parameters.

Acknowledgment. We are grateful to the Ministry of Education, Culture, and Science of the Japanese Government for the financial support of this research.

Note Added in Proof: After submission of this paper two reports on the (μ-η^1:η^1-ethynediyl)dimetal complex (μ-C_2)[$CpM(CO)_n$]$_2$ (M = W, n = 3;[28a] M = Ru, n = 2[28b]) appeared.

Supplementary Material Available: Tables of positional parameters of the hydrogen atoms, anisotropic thermal parameters, and all bond distances and angles for 4 and 5 (17 pages); tables of observed and calculated structure factors for 4 and 5 (36 pages). Ordering information is given on any current masthead page.

(28) (a) Tseng, T.-W.; Wu, I.-Y.; Lin, Y.-C.; Chen, C.-T.; Chen, M.-C.; Tsai, Y.-J.; Chen, M.-C.; Wang, Y. *Organometallics* **1991**, *10*, 43. (b) Koutsantonis, G. A.; Selegue, J. P. *J. Am. Chem. Soc.* **1991**, *113*, 2316. (c) See also: Ogawa, H.; Onitsuka, K.; Joh, T.; Takahashi, S.; Yamamoto, Y.; Yamazaki, H. *Organometallics* **1988**, *7*, 2257.

Analytical Study of a Series of Substituted (2,2′-Bipyridyl)(pentamethylcyclopentadienyl)rhodium and -iridium Complexes with Regard to Their Effectiveness as Redox Catalysts for the Indirect Electrochemical and Chemical Reduction of NAD(P)$^+$

Eberhard Steckhan,* Sabine Herrmann, Romain Ruppert, Eva Dietz, Markus Frede, and Elke Spika

Institut für Organische Chemie und Biochemie der Universität Bonn, Gerhard-Domagk-Strasse 1, D-5300 Bonn 1, FRG

Received July 12, 1990

The influence of the substituents in the 2,2′-bipyridine ligands of $[(C_5Me_5)Rh(bpy)(H_2O)]Cl_2$ complexes on their electrochemical behavior and their effectiveness as redox catalysts toward the chemical (using formate as donor) or indirect electrochemical reduction of NAD(P)$^+$ to NAD(P)H have been studied in detail. The electrochemically or chemically reduced complexes have been shown to act as hydride atom transfer agents. The intermediate rhodium hydride complex was identified by ^{1}H NMR spectroscopy by using 6,6′-dimethyl-2,2′-bipyridine as the ligand. The catalytic efficiency is decreased by electron-withdrawing substituents in the 2,2′-bipyridine ligand, while it is increased by electron-donating substituents. Because of steric effects, substituents in the 6-position of the ligand slow down the catalytic reaction. The formation of the rhodium hydride complexes by formate shows a Michaelis type kinetic behavior, if the formate concentration is varied while the hydride transfer to NAD$^+$ is zero order in NAD$^+$. A number of effective catalysts for the NAD(P)$^+$ reduction have thus been obtained.

Introduction

To a great extent, the reduced forms of nicotinamide adenine dinucleotide (NADH) or nicotinamide adenine dinucleotide phosphate (NADPH) are the hydride donors in enzymatic reductions. The application of enzymes as extraordinarily effective biocatalysts in organic synthesis is increasing. Reactions catalyzed by dehydrogenases are of special value for organic synthesis, because they possess high chemo-, regio-, and stereospecifity. Therefore an effective and broadly applicable regeneration method for NADH and NADPH is indispensable.

The most frequently used procedure is enzyme-catalyzed regeneration of NADH or NADPH.[1] A system for continuous production of amino acids with regeneration of NADH with formate catalyzed by formate dehydrogenase is technically already highly developed.[2] But these enzyme-coupled cofactor regeneration systems are rather complicated, because they include two enzymes, two products, and two substrates. Indirect electrochemical regeneration of NAD(P)H from NAD(P)$^+$ using methylviologen as mediator is shown to be possible under cocatalysis of special redox enzymes or microorganisms.[3] These enzymes are able to accept electrons from the me-

(1) Jones, J. B.; Beck, J. F. In *Application of Biochemical Systems in Organic Chemistry*; Jones, J. B., Sih, C. J., Perlman, D., Eds.; Wiley-Interscience: New York 1976; Part 1, pp 370-376. Jones, J. B. In *Enzymes in Organic Synthesis*; Porter, R., Clark, S., Eds.; Pitman: London 1985; p 3. Whitesides, G. M. *Ibid.*, p 76.

(2) Wandrey, C.; Wichmann, R.; Bückmann, A. F.; Kula, M. R. *Umschau* **1984**, *84*, 88. Wandrey, C.; Wichmann, R.; Berke, W.; Morr, M.; Kula, M. R. *Prepr.-Eur. Congr. Biotechnol., 3rd* **1984**, *3*, 239. Wandrey, C.; Wichmann, R. In *Enzymes and Immobilized Cells in Biotechnology*; Laskin, A. I., Ed.; Benjamin/Cummings: Menlo Park, CA, 1985; p 177. Kula, M. R.; Wandrey, C. *Methods Enzymol.* **1986**, *136*, 9.

(3) Ito, M.; Kuwana, T. *J. Electroanal. Chem. Interfacial Electrochem.* **1971**, *32*, 415. DiCosimo, R.; Wong, C.-H.; Daniels, L.; Whitesides, G. M. *J. Org. Chem.* **1981**, *46*, 4622. Shaked, Z.; Barber, J. J.; Whitesides, G. M. *J. Org. Chem.* **1981**, *46*, 4101. Simon, H. *GIT Fachz. Lab.* **1988**, *32*, 458. Simon, H.; Günther, H.; Bader, J.; Tischer, W. *Angew. Chem.* **1981**, *93*, 897. Simon, H.; Günther, H.; Bader, J.; Neumann, S. In *Enzymes in Organic Synthesis*; Porter, R., Clark, S., Eds.; Pitman: London, 1985; p 97. Bader, J.; Günther, H.; Neumann, S.; Thanos, I. *Angew. Chem., Int. Ed. Engl.* **1985**, *24*, 539. Skopan, H.; Günther, H.; Simon, H. *Angew. Chem., Int. Ed. Engl.* **1987**, *26*, 128. Thanos, J.; Bader, J.; Günther, H.; Neumann, S.; Krauss, F.; Simon, H. *Methods Enzymol.* **1986**, *136*, 302. Nagata, S.; Günther, H.; Bader, J.; Simon, H. *FEBS Lett.* **1987**, *210*, 66.

0276-7333/91/2310-1568$02.50/0

diator one by one and transfer them to NAD(P)$^+$ as a pair. But the systems also are complicated, as they also need two enzymes. In addition to that, the cofactor-regenerating enzymes like enoate reductase, lipoamide dehydrogenase, glutathione reductase, or ferredoxin NADP reductase are quite sensitive and not very stable.

A nonenzymatic electrochemical or chemical method for NAD(P)H regeneration would be principally of great importance. Direct cathodic reduction of NAD$^+$ is not suitable for NADH regeneration. At −0.9 V vs SCE, NAD dimers are generated. Reduction at −1.8 V vs SCE yields only 50–63% of the enzymatically active 1,4-NADH.[4] In another rather complicated cyclic process, recovery of NAD$^+$ from 1,6-NADH and the NAD dimers by anodic oxidation was tried. However, the losses are still very high.[5] Therefore electrochemical regenerations have to take place by an indirect pathway using redox catalysts, which act as hydride-transfer agents. The only chemical reducing agent that selectively reduces NAD(P)$^+$ to 1,4-NAD(P)H is dithionite.[6] Unfortunately, dithionite affects enzymes.[7]

Recently, we presented the rhodium complex aquo(2,2′-bipyridine)(pentamethylcyclopentadienyl)rhodium(III) (1) as an extremely effective redox catalyst for the indirect electrochemical regeneration of NADH[8] as well as for the chemical reduction of NAD(P)$^+$ with formate as hydride donor.[9,10] The system is advantageous, because it is uncomplicated and as effective for NAD$^+$ as for NADP$^+$. In order to find a system with highest reactivity toward NAD(P)H generation and to develop a complex with a suitable anchor group for binding it to polyethylene glycol,[10] we investigated a series of rhodium complexes with modified bipyridine ligands and a corresponding iridium complex (1–14) by cyclic voltammetry and UV spectroscopy. Cyclic voltammetry is a very powerful technique for studying the redox catalytic effectiveness of these complexes for the reduction of NAD(P)$^+$. Kölle et al. have already described some cyclic voltammograms of such rhodium complexes.[11,12]

Experimental Section

Instrumentation. Electrochemical measurements were made with an Amel (Milano) potentiostat Model 553 and a Kontron (München) function generator Model 8299 or a Cypress Systems (Lawrence, Kansas) CYSY-1H computer-controlled electroanalytical system in combination with a Hewlett-Packard Model 7440A Color-Pro digital plotter. Current–voltage curves were recorded on a Hewlett-Packard XY recorder Model 7045A. UV spectra were recorded on a Cary 219 spectrometer (Varian Associates, Palo Alto).

Chemicals. Rhodium trichloride hydrate (Degussa), iridium trichloride hydrate (Degussa), hexamethylbicyclo[2.2.0]hexa-2,5-diene (Aldrich), 2,2′-bipyridine (Aldrich), 1,10-phenanthroline (Aldrich), 4,4′-dimethyl-2,2′-bipyridine (Aldrich), 6,6′-dimethyl-2,2′-bipyridine (Fluka), nicotinamide adenine dinucleotide (Sigma), nicotinamide adenine dinucleotide phosphate (Sigma), and tris(hydroxymethyl)aminomethane (Serva) were used as received. The reagents 2,2′-bipyridine-4,4′-dicarboxylic acid,[13] 2,2′-bipyridine-4,4′-dicarboxylic acid diethyl ester,[14] 2,2′-bipyridine-5,5′-dicarboxylic acid diethyl ester,[15] 5-hydroxy-2,2′-bipyridine,[16] 5-acetoxy-2,2′-bipyridine,[16] 5-(bromomethyl)-2,2′-bipyridine,[17] bis(μ-chloro)dichlorobis(pentamethylcyclopentadienyl)dirhodium(III),[18] bis(μ-chloro)dichlorobis(pentamethylcyclopentadienyl)diiridium(III),[19] aquo(2,2′-bipyridine)(pentamethylcyclopentadienyl)iridium(III) dichloride[20] were prepared by literature methods. 4-Methyl-2,2′-bipyridine was prepared according to Huang and Brewer;[21] however the yield was improved from 20% to 65% by performing the reaction between 1-(2-pyridacyl)pyridinium iodide and 2-butenal in a ratio of 1:2 at 65 °C for 24 h. 5-(Ethoxymethyl)-2,2′-bipyridine was obtained by reaction of 5-(bromomethyl)-2,2′-bipyridine with sodium ethanolate and subsequent purification by column chromatography (silica gel, dichloromethane/methanol, 24:1). As an improvement to our former method,[10] 5-[poly(oxyethylene)methylene]-2,2′-bipyridine (PEG MW 20 000) was received in the following way. A 10-g (0.5 mmol) sample of polyethylene glycol (MW 20 000) was dried over P_2O_5 and dissolved in 1 L of THF, and the solution was refluxed for 24 h under argon atmosphere by using a water separator. After the addition of freshly pressed sodium (2 g, 87 mmol) and refluxing the solution for an additional 48 h at a maximum temperature of 80–90 °C, 1.5 g (6 mmol) of very dry 5-(bromomethyl)-2,2′-bipyridine was added under argon and refluxed for another 72 h at a maximum of 80 °C. After hot filtration from the unreacted sodium, the toluene phase was twice intensively extracted with water. The product was purified by dialysis (4 days, 6 times versus 10 L of bidistilled water, Servapor dialysis tubing). The dialysate was further purified by ultrafiltration (24 h) in a cell that was equipped with a YM-5 membrane (cutoff >5000 u). After freeze-drying, the lyophilate (6.3 g, 0.32 mmol, 63% yield with respect to applied polyethylene glycol) was characterized by UV spectroscopy. By comparison of the UV spectrum with that of 5-(ethoxymethyl)-2,2′-bipyridine [UV (0.05 M phosphate buffer, pH 3.0, 25 °C): λ_{max} = 242, 303 nm] an 85–87% yield of modified polyethylene glycol end groups could be calculated.

The rhodium complexes were prepared analogous to the procedure used by Kölle and Grätzel.[11,12] Further purification could be effected by dissolving the complex in methanol at room temperature, slow addition of diethyl ether until first crystallization appeared, and crystallization at 4 °C. The polyethylene glycol bound complex 11[10] was synthesized starting from 2 g (0.1 mmol) of 5-[poly(oxyethylene)methylene]-2,2′-bipyridine (PEG MW 20 000) (corresponding to 1.7 mmol of active bipyridine end groups based on 85% bipyridine-modified end groups) dissolved in 500 mL of absolute methanol by addition of 400 mg (0.65 mmol) of bis(μ-chloro)dichlorobis(pentamethylcyclopentadienyl)dirhodium(III) and stirring for 18 h under argon. Water (500 mL) was then added, and most of the organic solvent was removed in vacuo at only slightly elevated temperature. The product was purified by dialysis (4 days, 6 times versus 10 L of bidistilled water, Servapor dialysis tubing). The dialysate was further purified by

(4) Ke, B. *J. Am. Chem. Soc.* **1956**, *78*, 3649. Ke, B. *Arch. Biochem. Biophys.* **1956**, *60*, 505. Powning, R. F.; Kratzing, C. C. *Arch. Biochem. Biophys.* **1957**, *66*, 249. Kono, T. *Bull. Agric. Chem. Soc. Jpn.* **1957**, *21*, 155. Kono, T.; Nakamura, S. *Bull. Agric. Chem. Soc. Jpn.* **1958**, *22*, 399. Burnett, J.; Underwood, A. L. *Biochemistry* **1965**, *4*, 2060. Cunningham, A. J.; Underwood, A. L. *Arch. Biochem. Biophys.* **1966**, *117*, 88. Cunningham, A. J.; Underwood, A. L. *Biochemistry* **1967**, *6*, 266. Burnett, R. W.; Underwood, A. L. *Biochemistry* **1968**, *7*, 3328. Janik, B.; Elving, P. J. *Chem. Rev.* **1968**, *68*, 295. Schmakel, C. O.; Santhanam, K. S. V.; Elving, P. J. *J. Am. Chem. Soc.* **1975**, *97*, 5083. Jaegfeldt, H. *Bioelectrochem. Bioenerg.* **1981**, *8*, 355.

(5) Drakesmith, F. G.; Gibson, B. *J. Chem. Soc., Chem. Commun.* **1988**, 1493.

(6) Jones, J. B.; Snedoon, D. W.; Higgins, W.; Lewis, A. J. *J. Chem. Soc., Chem. Commun.* **1972**, 856.

(7) Ramio, R. Lilius, E.-M. *Enzymologia* **1971**, *10*, 360.

(8) Ruppert, R.; Herrmann, S.; Steckhan, E. *Tetrahedron Lett.* **1987**, *28*, 6583.

(9) Ruppert, R.; Herrmann, S.; Steckhan, E. *J. Chem. Soc., Chem. Commun.* **1988**, 1150.

(10) Steckhan, E.; Herrmann, S.; Ruppert, R.; Thömmes, J.; Wandrey, C. *Angew. Chem., Int. Ed. Engl.* **1990**, *29*, 388.

(11) Kölle, U.; Grätzel, M. *Angew. Chem., Int. Ed. Engl.* **1987**, *26*, 567.

(12) Kölle, U.; Kang, B.-S.; Infelta, P.; Comte, P.; Grätzel, M. *Chem. Ber.* **1989**, *122*, 1869.

(13) Bos, K. D.; Kraaijkamp, J. G.; Noltes, J. G. *Synth. Commun.* **1979**, *9*, 497. Elliott, C. M.; Hershenhart, E. J. *J. Am. Chem. Soc.* **1982**, *104*, 7519.

(14) Sprintschnik, G.; Sprintschnik, H. W.; Kirsch, P. P.; Whitten, D. G. *J. Am. Chem. Soc.* **1977**, *99*, 4947.

(15) Grammenudi, S.; Franke, M.; Vögtle, F.; Steckhan, E. *J. Incl. Phenom.* **1987**, *5*, 695.

(16) Pirzada, N. H.; Pojer, P. M.; Summers, L. A. *Z. Naturforsch.* **1976**, *31B*, 115.

(17) Eaves, J. G.; Munro, H. S.; Parker, D. *Inorg. Chem.* **1987**, *26*, 644.

(18) Booth, B. L.; Haszeldine, R. N.; Hill, M. *J. Chem. Soc. A* **1969**, 1299.

(19) Kang, J. W.; Moseley, K.; Maitlis, P. M. *J. Am. Chem. Soc.* **1969**, *91*, 5970.

(20) Ziessel, R. *J. Chem. Soc., Chem. Commun.* **1988**, 16.

(21) Huang, T. L.; Brewer, D. G. *Can. J. Chem.* **1981**, *59*, 1689.

ultrafiltration (24 h) in a cell that was equipped with a YM-5 membrane (cutoff >5000 u). After freeze-drying the intensely yellow solution, the cotton-wool-like yellow lyophilate (1.65 g, 0.083 mmol, 82.5% yield with respect to applied PEG (MW 20000) bpy) was characterized by UV spectroscopy. By comparison of the UV spectrum with that of $[(C_5Me_5)Rh(bpy\text{-}5\text{-}CH_2OEt)(H_2O)]Cl_2$ (**10**) [UV (0.1 M Tris/HCl buffer, pH 7.5, 25 °C): λ_{max} = 234, 308, 316 nm] an 83–88% yield of rhodium complex modified ethylene glycol end groups could be calculated.

Analytical Data

5-(Ethoxymethyl)-2,2′-bipyridine. ^{1}H NMR (60 MHz, $CDCl_3$, TMS_{int}), ppm: δ 1.26 (t, 3 H, J = 7 Hz), 3.57 (q, 2 H, J = 7 Hz), 4.53 (s, 2 H), 7.07–8.73 (m, 7 H). MS (70 eV, 300 μA), m/z (%) [assignment]: 214 (42) [M^+] 185 (28) [M^+ – Et], 169 (100) [M^+ – OEt], 157 (55) [bpy + H], 141 (22), 115 (5), 78 (13) [Py], 51 (8). UV (H_2O, pH 3.0, 25 °C), nm (ε, L·mol^{-1}·cm^{-1}): λ_{max} 242, 304 (8900, 1680).

$\{[(C_5Me_5)Rh(\mu\text{-}Cl)Cl]_2\}$. Anal. Calcd for $C_{20}H_{30}Cl_4Rh_2$ (618.08): C, 38.86; H, 4.89. Found: C, 38.80; H, 4.61.

$[(C_5Me_5)Rh(bpy)(H_2O)]Cl_2$ (1). ^{1}H NMR (60 MHz, D_2O), ppm: δ 1.47 (s, 15 H), 7.60–8.93 (m, 8 H). UV (H_2O, pH 7.5, 25 °C), nm (ε, L·mol^{-1}·cm^{-1}): λ_{max} 231, 313, 232, 370 (27800, 11900, 2100). Anal. Calcd for $C_{20}H_{25}N_2OCl_2Rh$ (483.24): C, 49.71; H, 5.21; N, 5.80. Found: C, 49.66; H, 5.20; N, 5.76.

$[(C_5Me_5)Rh(phen)(H_2O)]Cl_2\cdot H_2O$ (2). ^{1}H NMR (60 MHz, D_2O), ppm: δ 1.83 (s, 15 H), 8.01–9.47 (m, 8 H). UV (H_2O, pH 7.5, 25 °C), nm (ε, L·mol^{-1}·cm^{-1}): λ_{max} 227, 274, 354 (34600, 31000, 2700). Anal. Calcd for $C_{22}H_{27}N_2O_2Cl_2Rh$ (525.28): C, 50.31; H, 5.18; N, 5.33. Found C, 50.67; H, 4.93; N, 5.06.

$[(C_5Me_5)Rh(4,4'\text{-}Me_2bpy)(H_2O)]Cl_2$ (3). ^{1}H NMR (60 MHz, D_2O), ppm: δ 1.60 (s, 15 H), 2.47 (s, 6 H), 7.57 (dd, 2 H, J = 6 Hz, J = 1.6 Hz), 8.07 (d, 2 H, J = 1.6 Hz), 8.70 (d, 2 H, J = 6 Hz). UV (H_2O, pH 7.5, 25 °C), nm (ε, L·mol^{-1}·cm^{-1}): λ_{max} 209, 232, 301, 309, 365 (29500, 35800, 13200, 13600, 2400). Anal. Calcd for $C_{22}H_{27}N_2OCl_2Rh$ (511.30): C, 51.68; H, 5.72; N, 5.48. Found: C, 51.17; H, 5.68; N, 5.56.

$[(C_5Me_5)Rh(6,6'\text{-}Me_2bpy)(H_2O)]Cl_2\cdot H_2O$ (4). ^{1}H NMR (60 MHz, D_2O), ppm: δ 1.4 (s, 15 H), 2.93 (s, 6 H), 7.3–8.2 (m, 6 H). UV (H_2O, pH 7.5, 25 °C), nm (ε, L·mol^{-1}·cm^{-1}): λ_{max} 237, 320, 328 (21378, 13489, 14125). Anal. Calcd for $C_{22}H_{31}N_2O_2Cl_2Rh$ (529.32): C, 51.17; H, 5.56; N, 5.68. Found: C, 51.15; H, 5.56; N, 5.42.

$\{(C_5Me_5)Rh[bpy\text{-}4,4'\text{-}(COOH)_2](H_2O)\}Cl_2\cdot H_2O$ (5). ^{1}H NMR (60 MHz, D_2O), ppm: δ 1.55 (s, 15 H), 8.15 (dd, 2 H, J = 6 Hz, J = 1.6 Hz), 8.80 (d, 2 H, J = 1.6 Hz), 9.00 (d, 2 H, J = 6 Hz). UV (H_2O, pH 7.5, 25 °C), nm (ε, L·mol^{-1}·cm^{-1}): λ_{max} 233, 315, 326 (42350, 14050, 14250). Anal. Calcd for $C_{22}H_{27}N_2O_6Cl_2Rh$ (589.28): C, 44.84; H, 4.62; N, 4.75. Found: C, 44.98; H, 4.56; N, 5.12.

$\{(C_5Me_5)Rh[bpy\text{-}4,4'\text{-}(COOEt)_2](H_2O)\}Cl_2$ (6). ^{1}H NMR (60 MHz, D_2O), ppm: δ 1.43 (t, 3 H, J = 6 Hz), 1.67 (s, 15 H), 4.50 (q, 2 H, J = 6 Hz), 8.23 (dd, 2 H, J = 6 Hz, J = 1.6 Hz), 8.77 (d, 2 H, J = 1.6 Hz), 9.03 (d, 2 H, J = 6 Hz). UV (H_2O, pH 7.5, 25 °C), nm (ε, L·mol^{-1}·cm^{-1}): λ_{max} 235, 320, 331 (42300, 13100, 13500). Anal. Calcd for $C_{26}H_{33}N_2O_5Cl_2Rh$ (627.37): C, 49.78; H, 5.30; N, 4.47. Found: C, 49.92; H, 5.24; N, 4.42.

$\{(C_5Me_5)Rh[bpy\text{-}5,5'\text{-}(COOEt)_2](H_2O)\}Cl_2$ (7). ^{1}H NMR (200 MHz, $CDCl_3$), ppm: δ 1.41 (t, 6 H, J = 7.5 Hz), 1.73 (s, 15 H), 4.46 (q, 4 H, J = 7.5 Hz), 8.78 (dd, 2 H, J = 9 Hz, J = 2.7 Hz), 9.29 (d, 2 H, J = 2.7 Hz), 9.54 (d, 2 H, J = 9 Hz). UV (H_2O, pH 7.5, 25 °C), nm (ε, L·mol^{-1}·cm^{-1}): λ_{max} 234, 313, 327 (25100, 19800, 20800). Anal. Calcd for $C_{26}H_{33}N_2O_5Cl_2Rh$ (627.37): C, 49.78; H, 5.30; N, 4.47. Found: C, 49.71; H, 5.00; N, 4.62.

$[(C_5Me_5)Rh(bpy\text{-}5\text{-}OH)Cl]Cl$ (8). ^{1}H NMR (60 MHz, D_2O), ppm: δ 1.63 (s, 15 H), 7.33–8.83 (m, 7 H). UV (H_2O, pH 7.5, 25 °C), nm (ε, L·mol^{-1}·cm^{-1}): λ_{max} 235, 327, 360 (23000, 12300, 11800). Anal. Calcd for $C_{20}H_{23}N_2OCl_2Rh$ (481.23): C, 49.92; H, 4.82; N, 5.82. Found: C, 49.77; H, 4.94; N, 5.82.

$[(C_5Me_5)Rh(bpy\text{-}5\text{-}OAc)(H_2O)]Cl_2$ (9). ^{1}H NMR (90 MHz, $CDCl_3$), ppm: δ 1.67 (s, 15 H), 2.36 (s, 3 H), 7.67–9.29 (m, 7 H). UV (H_2O, pH 7.5, 25 °C), nm (ε, L·mol^{-1}·cm^{-1}): λ_{max} 233, 306, 358 (25600, 13600, 11500). Anal. Calcd for $C_{22}H_{27}N_2O_3Cl_2Rh$ (541.28): C, 48.82; H, 5.03; N, 5.18. Found: C, 49.31; H, 4.90; N, 5.76.

$[(C_5Me_5)Rh(bpy\text{-}5\text{-}CH_2OEt)(H_2O)]Cl_2$ (10). ^{1}H NMR (60 MHz, D_2O), ppm: δ 1.23 (t, 3 H, J = 7 Hz), 1.58 (s, 15 H), 3.63 (q, 2 H, J = 7 Hz), 7.57–8.97 (m, 7 H). UV (H_2O, pH 7.5, 25 °C), nm (ε, L·mol^{-1}·cm^{-1}): λ_{max} 233, 308, 318 (31600, 15300, 15700). Anal. Calcd for $C_{23}H_{31}N_2O_2Cl_2Rh$ (541.32): C, 51.03; H, 5.77; N, 5.18. Found: C, 51.55; H, 5.65; N, 5.45.

$\{(C_5Me_5)Rh[bpy\text{-}5\text{-}CH_2O(PEG)](H_2O)\}Cl_2$ (PEG MW 20000) (11). UV (H_2O, pH 7.5, 25 °C), nm (ε, L·mol^{-1}·cm^{-1}): λ_{max} = 233, 308, 318. 83–88% rhodium complex modified end groups determined by UV spectroscopy using **10** as a standard.

$[(C_5Me_5)Rh(4\text{-}Mebpy)(H_2O)]Cl_2\cdot 2H_2O$ (12). ^{1}H NMR (60 MHz, D_2O), ppm: δ 1.70 (s, 15 H), 2.63 (s, 3 H), 7.6 (d, 1 H, J = 5.6 Hz), 7.8 (dd, 1 H, J = 7.8, J = 5.6 Hz), 8.21 (dd, 1 H, J = 8.4, J = 7.8), 8.67 (d, 1 H, J = 5.6), 8.79 (s, 1 H), 8.83 (d, 1 H, J = 5.6), 8.9 (d, 1 H, J = 8.4). UV (H_2O, pH 7.5, 25 °C), nm (ε, L·mol^{-1}·cm^{-1}): λ_{max} = 229, 301, 310, 350 (30903 shoulder, 13183, 12882, 24547). Anal. Calcd for $C_{21}H_{31}N_2O_3Cl_2Rh$ (533.301): C, 47.30; H, 5.86; N, 5.25. Found: C, 47.05; H, 5.82; N, 5.97.

$[(C_5Me_5)Rh(dmg)Cl]Cl$ (13). ^{1}H NMR (60 MHz, D_2O), ppm: δ 1.70 (s, 15 H), 2.28 (s, 6 H). UV (H_2O, pH 7.5, 25 °C), nm (ε, L·mol^{-1}·cm^{-1}): λ_{max} = 249 (23100). Anal. Calcd for $C_{14}H_{23}N_2O_2Cl_2Rh$ (425.16): C, 39.55; H, 5.45; N, 6.59. Found: C, 38.96; H, 5.61; N, 6.79.

$\{[(C_5Me_5)Ir(\mu\text{-}Cl)Cl]_2\}$. Anal. Calcd for $C_{20}H_{30}Cl_4Ir_2$ (796.71): C, 30.15; H, 3.80. Found: C, 30.49; H, 3.89.

$[(C_5Me_5)Ir(bpy)(H_2O)]Cl_2$ (14). ^{1}H NMR (60 MHz, D_2O), ppm: δ 1.62 (s, 15 H), 7.56–8.95 (m, 8 H). UV (H_2O, pH 7.5, 25 °C), nm (ε, L·mol^{-1}·cm^{-1}): λ_{max} 244, 292, 305, 317 (12750, 11450, 11400, 10650) Anal. Calcd for $C_{20}H_{25}N_2OCl_2Ir$ (572.56): C, 41.96; H, 4.40; N, 4.89. Found: C, 42.21; H, 4.53; N, 5.02.

Procedures

Cyclic Voltammetry. An undivided Metrohm electrolysis cell Model EA 875-5 of 50-mL volume, a Metrohm glassy carbon disk electrode (A = 7.1 mm^2), as the cathode, a Pt wire as the anode, and a saturated Ag/AgCl reference electrode were used. The cathode was polished with a slurry of 0.3-μm alumina on a tissue before each series of cyclic voltammograms. The supporting electrolyte was 0.1 M Tris adjusted to pH 7.5 with HCl, unless specified otherwise. Prior to measurements, solutions were deoxygenated by purging with Ar gas for 15 min. During measurements, a stream of Ar was passed over the solution. Some potential sweeps were done in the potential range immediately prior to recording a group of cyclic voltammograms. All experiments were carried out at room temperature. For each series of cyclic voltammograms, with the exception of the pH-dependent studies, the background current was recorded and background current corrections were performed. Most of the cyclic voltammograms were proofed by a second measurement.

UV Spectroscopic Study of the Rhodium(III) Complex Reaction with Formate. A sodium phosphate (0.1 M) buffer solution of pH 7.0 containing sodium formate (0.5 M) and NAD^+, or PEG–NAD^+ (3.8×10^{-4} M or 7.6×10^{-4} M) was freed from oxygen by an argon stream during 15 min. A 1.5-mL aliquot of the solution was transfered to the cuvette by using a Hamilton syringe, which also was purged with argon. The immediately closed cuvette was than brought to the desired temperature by thermostating for 40–60 min in the UV spectrometer. Then, 7.5 μL of a 5×10^{-3} M stock solution of the complex in water was added with a syringe, quickly mixed with the buffer, and the absorbance increase at 340 nm immediately recorded. The thereby induced volume change was taken into account for the calculation of the turnover frequency (TF).

$$TF = \frac{A_{340}}{\epsilon d c_{Rk} t}\ (h^{-1})$$

TF = turnover frequency (h^{-1})

A_{340} = absorbance at 340 nm

ε = molar absorptivity of NAD(P)H at its characteristic band at 340 nm (6230 L·mol^{-1}·cm^{-1})

d = optical path length (cm)

t = reaction time (h)

c_{Rk} = concentration of the catalyst (mol·L^{-1})

Results and Discussion

Cyclic Voltammograms in the Absence of NAD(P)$^+$. The cyclic voltammograms of $[(C_5Me_5)Rh(4,4'$-

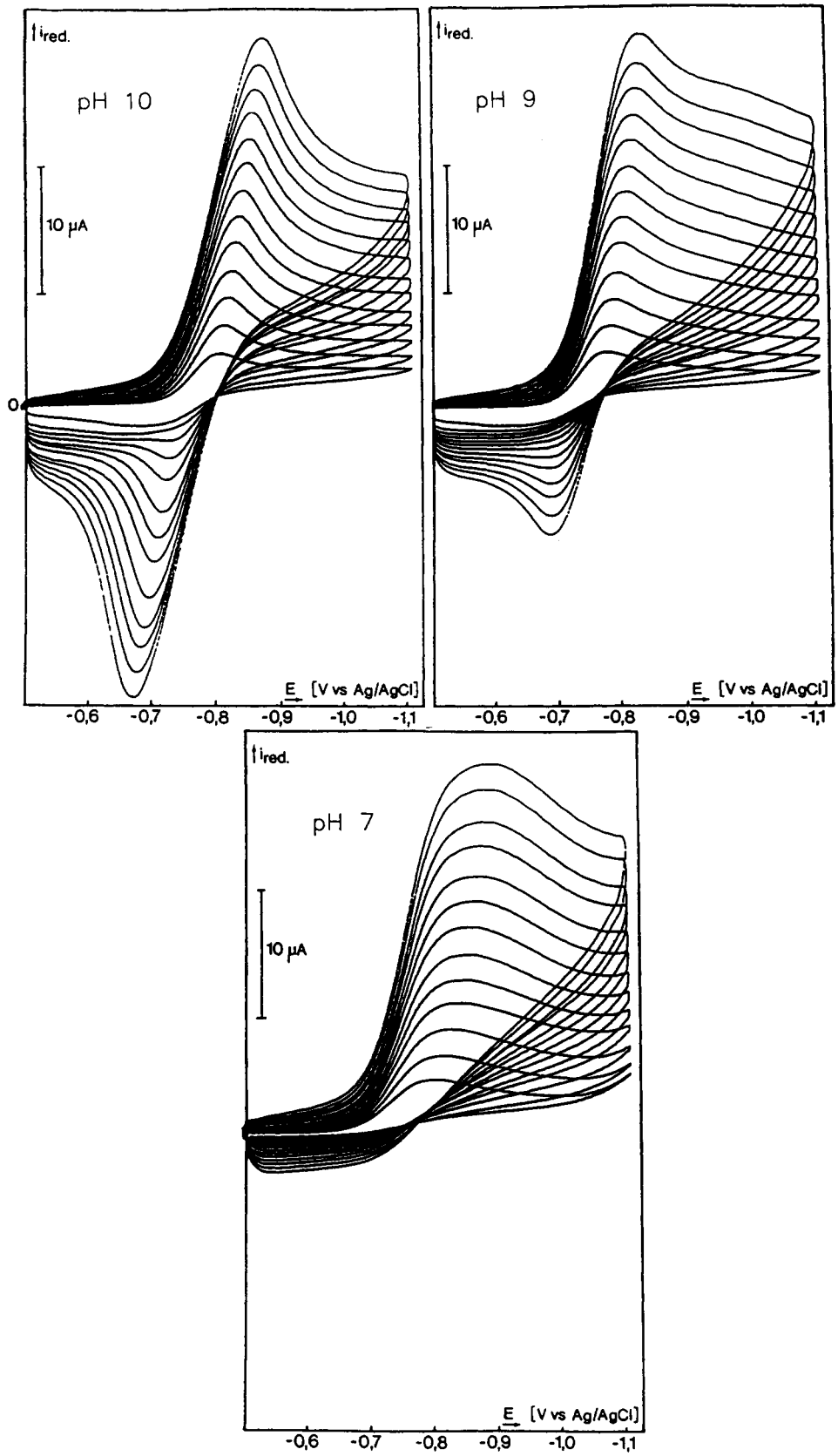

Figure 1. pH dependence (pH 10, 9, 7) of the cyclic voltammograms of complex **3** (5×10^{-4} M) in 0.1 M Tris/HCl buffer at a glassy carbon cathode (v = 9, 25, 49, 81, 121, 169, 225, 289, 361, 441, 529, 625, 729 mV/s).

$Me_2bpy)(H_2O)]Cl_2$ (**3**) in Tris/HCl buffer at the pH values 10, 9, and 7 are represented in Figure 1. At pH 10, disregarding a rather large uncompensated iR drop, the system has an almost reversible character, while at pH 7 and 9, a relatively broad double reduction peak is observed. By calibration of the current for the cyclic voltammogram at pH 10 with an electrochemically reversible one-electron system, a two-electron wave could be determined. ($E_{pc} - E_{pa}$) and ($E_{pc} - E_{pc/2}$) values were corrected for the uncompensated iR drop by plotting them versus the square root of the potential scan rate and extrapolating the thus obtained straight lines toward a scan rate of zero. In both

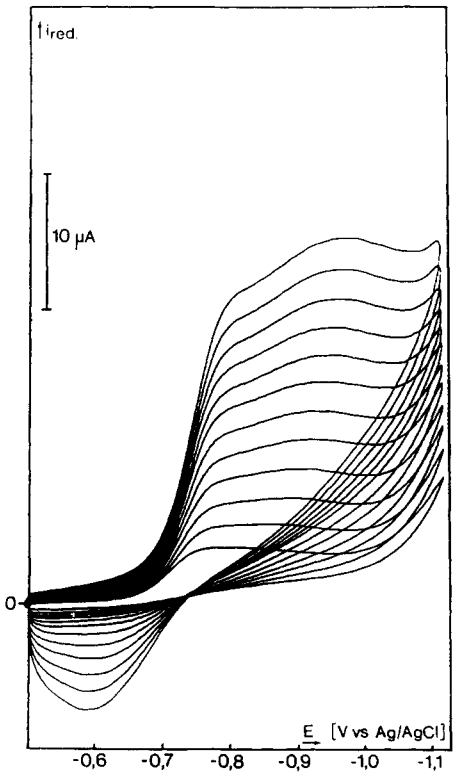

Figure 2. Cyclic voltammogram of complex **2** (5×10^{-4} M) in 0.1 M Tris/HCl buffer (pH 7.5) at a glassy carbon cathode (v = 9, 25, 49, 81, 121, 169, 225, 289, 361, 441, 529, 625, 729 mV/s).

cases, a value of 50 mV was obtained. This corresponds to theoretical cyclic voltammograms for the case of electrochemically and chemically reversible closely spaced two-electron-transfer reactions calculated by Polcyn, Myers, and Shain.[22a] For a value of 50 mV for ($E_{pc} - E_{pc/2}$), the standard potential of the second electron transfer must be about 25 mV more negative than the one of the first electron transfer. The peak current ratio at ($i_{p,ox}/i_{p,red}$) at pH 10 is 1. The reduction peak current ($i_{p,red}$) shows a linear dependence on the square root of the potential sweep rate ($\sqrt{v}$).

With decreasing pH value a relatively broad double reduction peak develops and the oxidation peak decreases remarkably (Figure 1). This can be explained by the fact that the Rh(I) complex takes up a proton in its ligand sphere forming the corresponding hydride complex[11] so that the Rh(I) complex is no longer available on the reverse potential sweep. The electrochemical behavior can thus be explained by eqs 1–5. By pulse radiolytic measurements, rate constants k_4 for the disproportionation step and k_5 for the protonation of the rhodium(I) complex have been determined.[12] At pH 7.5, values of 3.7×10^8 $s^{-1} \cdot mol^{-1}$ for k_4 and 10.6 s^{-1} for k_5 were obtained.

$$[(C_5Me_5)Rh^{III}(bpy)L]^{2+} + e^- \rightleftharpoons [(C_5Me_5)Rh^{II}(bpy)L]^+ \quad E_1 \quad (1)$$

$$[(C_5Me_5)Rh^{II}(bpy)L]^+ \rightleftharpoons [(C_5Me_5)Rh^{II}(bpy)]^+ + L \quad (2)$$

$$[(C_5Me_5)Rh^{II}(bpy)L]^+ + e^- \rightleftharpoons (C_5Me_5)Rh^{I}(bpy) + L \quad E_2 \quad (3)$$

or $$[(C_5Me_5)Rh^{II}(bpy)]^+ + e^- \rightleftharpoons (C_5Me_5)Rh^{I}(bpy)$$

$$[(C_5Me_5)Rh^{II}(bpy)L]^+ + [(C_5Me_5)Rh^{II}(bpy)]^+ \overset{k_4}{\rightleftharpoons} (C_5Me_5)Rh^{I}(bpy) + [(C_5Me_5)Rh^{III}(bpy)L]^{2+} \quad (4)$$

$$(C_5Me_5)Rh^{I}(bpy) + H^+ \overset{k_5}{\rightleftharpoons} [(C_5Me_5)Rh^{III}H(bpy)]^+ \quad (5)$$

Table I. Cathodic Peak and Half-Peak Potentials from the Cyclic Voltammograms of $[Cp^*RhL'L]^{2+}$ Complexes in 0.1 M Tris/HCl Buffer (pH 7.5) at a Glassy Carbon Cathode at a Scan Rate of 9 mV/s

complex	L'	E_p, mV	$E_{p/2}$, mV	$E_{p/2} - E_p$, mV
1	bpy	−760	−690	70
2	phen	−745	−675	70
3	4,4′-Me_2bpy	−840	−720	120
4	6,6′-Me_2bpy	−920	−885	65
5	bpy-4,4′-$(COOH)_2$	−845	−660	185
8	bpy-5-OH	−900	−730	170
9	bpy-5-OAc	−900	−725	175
10	bpy-5-CH_2OEt	−820	−690	130
12	4-Mebpy	−735	−690	45

Complexes **1**, **2**, **4**, **5**, and **8**–**12** (bidentate ligands: bpy, phen, 6,6′-Me_2bpy, bpy-4,4′-$(COOH)_2$, bpy-5-OH, bpy-5-OAc, bpy-5-CH_2OEt, bpy-5-CH_2O(PEG), 5-Mebpy) result in similar cyclic voltammograms. In the cyclic voltammogram of $[(C_5Me_5)Rh(phen)(H_2O)]Cl_2$ (**2**), the double reduction peak is clearly developed (Figure 2). At high-potential sweep rates (v) both reduction steps (eqs 1 and 3) can be recognized. But with decreasing v, the second wave for the reduction of the rhodium(II) complex (eq 3) is diminished, because the disproportionation of the Rh(II) complex (eq 4) has a larger time window to occur. If a D_2O–Tris/HCl buffer is used, the cyclic voltammogram of complex **1** shows a distinct increase of the reversibility as compared with the H_2O system under otherwise identical conditions. At the same time, the catalytic effectiveness toward $NAD(P)^+$ reduction (see below) is reduced. These observations are in support of the assumption that the protonation of the rhodium(I) complex (eq 5) is the rate-determining step.

For compounds **1**–**5** and **8**–**10** the $i_{p,red}/\sqrt{v}$ values decrease with increasing potential sweep rate starting from the lower end of the sweep rates (9–121 mV/s) but become constant for higher potential sweep rates. This is in accordance with a disproportionation reaction, as shown in the case of the tetraphenylethylene oxidation.[22b] The higher $i_{p,red}/\sqrt{v}$ values at low-potential sweep rates are not caused by hydrogen evolution, because the reduction peak current ($i_{p,red}$) is linearly dependent on the square root of the potential sweep rate ($\sqrt{v}$).

Because of the interfering disproportionation reaction and the exchange of the monodentate ligand, an exact determination of the reduction potential is not possible. As measures for the reducibility of the complexes for later potential-controlled electrolysis, we determined the reduction peak potential ($E_{p,red}$) and reduction half-peak potential ($E_{p,red/2}$, at $i_{p,red/2}$) for the potential sweep rate 9 $mV \cdot s^{-1}$. At such slow sweep rates, the influence of uncompensated iR drop is also diminished. These values are listed in Table I. The difference ($E_{p,red} - E_{p,red/2}$) indicates the broadness of the reduction peaks. Electron-withdrawing substituents at the bipyridine ligand cause lower electron density at the rhodium central atom and ease the reduction of Rh(III). The reduction potential shifts anodically. Electron-donating substituents cause a cathodic shift of the reduction peak potential.

On the reverse potential sweep in the cyclic voltammograms of complexes **1**, **3**, **4**, **8**–**10**, and **12** (bidentate ligands: bpy, 4,4′-Me_2bpy, 6,6′-Me_2bpy, bpy-5-OH, bpy-5-OAc, bpy-5-CH_2OEt, 4-Mebpy) in tris/HCl buffer at the pH value 7.5, no or only a very small (**12**) oxidation peak is developed. The Rh(I) complex is almost totally consumed

(22) (a) Polcyn, D. S.; Shain, I. *Anal. Chem.* **1966**, *38*, 370. Myers, R. L.; Shain, I. *Anal. Chem.* **1969**, *41*, 980. (b) Stuart, J. D.; Ohnesorge, W. E. *J. Am. Chem. Soc.* **1971**, *93*, 4531.

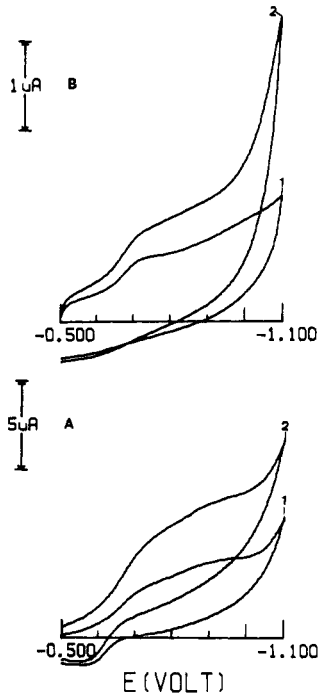

Figure 3. Cyclic voltammograms of complexes **10** (1.0 mM) (A) and **11** (1 mM) (B) in 0.1 M Tris/HCl buffer (pH 7.5) using a glassy carbon cathode (1 mm o.d.) and a Ag/AgCl reference electrode at a scan rate of 289 mV/s. Curves 1 in the absence and curves 2 in the presence of NAD^+ (1.0 mM).

under formation of the corresponding hydride complex in the time domain of the cyclic voltammogram. The same is true for the PEG (MW 20000) bound complex **11** (Figure 3). Figure 3 compares the cyclic voltammogram of **11** with that of **10** in the absence and presence of NAD^+. The high molecular weight complex shows an almost identical reduction potential. The current, however, is decreased by a factor of more than 4. This cannot only be explained by the lower diffusion coefficient, which could only account for a factor of about 2 in the current. Therefore it is assumed that the conformation of the polyethylene glycol reduces the accessibility of the rhodium complex end groups. The same behavior was observed in the case of a polyethylene glycol bound ferrocene derivative.[23] In the case of $[(C_5Me_5)Rh(phen)(H_2O)]Cl_2$ (**2**) a small oxidation peak appears (Figure 2). In the cyclic voltammogram of $\{(C_5Me_5)Rh[bpy\text{-}4,4'\text{-}(COOH)_2](H_2O)\}Cl_2$ (**5**) the oxidation peak is even more developed and has a desorption peak superpositioned on it. The peak current ratio $i_{p,ox}/i_{p,red}$ for v = 729 mV·s^{-1} is 1.2. This behavior indicates that in these cases the corresponding hydride complex is generated relatively slowly.

The cyclic voltammograms of the complexes $\{(C_5Me_5)Rh[bpy\text{-}4,4'\text{-}(COOEt)_2](H_2O)\}Cl_2$ (**6**) and $\{(C_5Me_5)Rh[bpy\text{-}5,5'\text{-}(COOEt)_2](H_2O)\}Cl_2$ (**7**), which are rather similar, show a double reduction peak at −0.55 V (Figure 4). The reduction peak current ($i_{p,red}$) is linearly dependent on $\sqrt{v}$. The electron transfer is diffusion controlled. On the reverse potential sweep an oxidation peak appears, which is also superpositioned by a desorption peak of presumably the neutral compound $\{(C_5Me_5)Rh^I[bpy\text{-}(COOEt)_2]\}$. The system is chemically largely reversible. If cyclic voltammograms are recorded in unbuffered H_2O instead of Tris/HCl buffer, also most of the other complexes show strong desorptive oxidation waves on the reverse potential sweep. The cyclic voltammogram of $[(C_5Me_5)Rh(dmg)$-

(23) Frede, M. Diploma thesis, Universität Bonn, 1990.

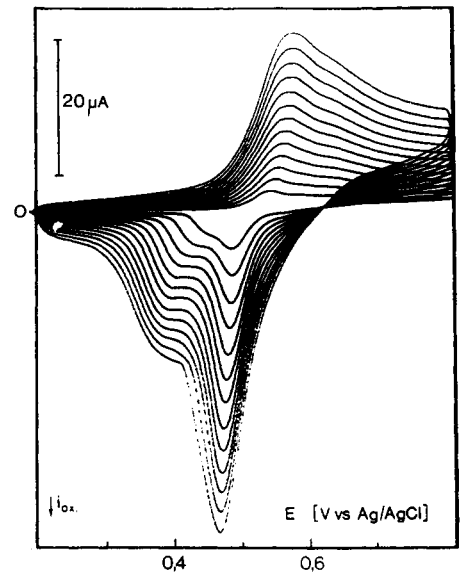

Figure 4. Cyclic voltammogram of complex **7** in 0.1 M Tris/HCl buffer (pH 7.5) at a glassy carbon cathode (v = 9, 25, 49, 81, 121, 169, 225, 289, 361, 441, 529, 625, 729 mV/s).

Cl]Cl (**13**) shows a reduction peak at −1 V and a small oxidation peak at −0.65 V. **13** is not suitable as a redox catalyst for $NAD(P)^+$ reduction, because at −1 V, NAD dimers are already cathodically generated.[24]

The iridium complex $[(C_5Me_5)Ir(bpy)(H_2O)]Cl_2$ (**14**) shows a cyclic voltammogram that is very similar to the one for $[(C_5Me_5)Rh(bpy)(H_2O)]Cl_2$ (**1**). At the potential sweep rate 9 mV·s^{-1} the values for the reduction peak potential ($E_{p,red}$) and the reduction half-peak potential ($E_{p,red/2}$) are −0.91 and −0.82 V, respectively. The reduction peak current ($i_{p,red}$) is linearly dependent on the square root of the potential sweep rate ($\sqrt{v}$). The Ir(II) complex also undergoes a slow disproportionation reaction, which is indicated by the $i_{p,red}/\sqrt{v}$ values, which are higher for low-potential sweep rates and become constant for high sweep rates. On the reverse potential sweep no oxidation peak appears. This indicates that the corresponding hydride complex is generated. This is also supported by the fact that the reduced iridium complex transfers hydride to carbonyl groups.

Cyclic Voltammograms in the Presence of $NAD(P)^+$ and PEG–NAD^+. Electrocatalytic processes in which the electroactive compound is regenerated within a homogeneous chemical redox reaction (eqs 6 and 7) can easily be detected by cyclic voltammetry.

$$A \pm e^- \rightleftharpoons B \quad \text{electrochemical reaction} \qquad (6)$$

$$B + C \rightarrow A + D \quad \text{homogeneous chemical reaction} \qquad (7)$$

For such a mechanism the peak current for A should be enhanced by the amount of the catalytic current while that for B should be decreased. At low sweep rates and very fast homogeneous reactions, the forward peak current should be proportional to the concentration (A + C) as the maximum limit while the peak for B on the reverse scan should be eliminated. The catalytic efficiency of a redox mediator toward a certain substrate is thus easily determined by measurement of the catalytic peak current increase.

We have already demonstrated the catalytic activity of the rhodium complex **1** with an unsubstituted 2,2′-bipyridine ligand for the indirect electrochemical reduction

(24) Franke, M.; Steckhan, E. *Angew. Chem., Int. Ed. Engl.* **1988**, *27*, 265. Wienkamp, R.; Steckhan, E. *Angew. Chem., Int. Ed. Engl.* **1982**, *21*, 782. *Angew. Chem. Suppl.* **1982**, 1739.

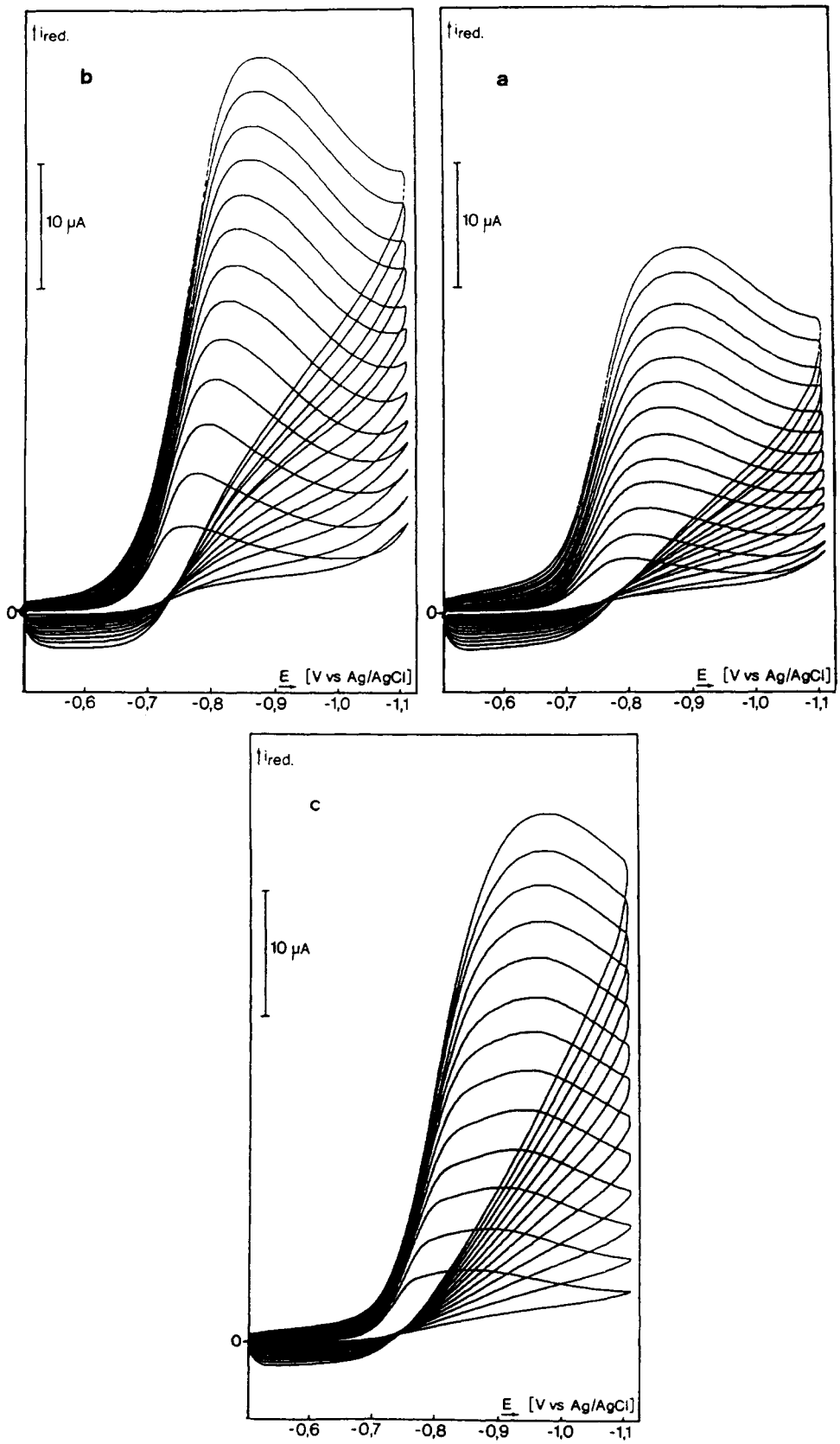

Figure 5. Cyclic voltammograms of complex **3** (5×10^{-4} M) in the absence (a) and presence of $NADP^+$ (5×10^{-4} M) (b), respectively, and in the presence of PEG–NAD^+ (5×10^{-4} M in NAD^+ end groups) (c) at a glassy carbon cathode in 0.1 M Tris/HCl buffer (pH 7.5) (v = 9, 25, 49, 81, 121, 169, 225, 289, 361, 441, 529, 625, 729 mV/s).

of NAD^+ by cyclic voltammetry as well as in potential-controlled electrolysis for the NADH formation and coupling to enzymatic reactions.[8] The cyclic voltammograms of **1–3**, **5**, and **10–12** in the absence and presence of NAD^+ are all very similar and equal that of complex **3** in the absence and presence of $NADP^+$ or polyethylene glycol (MW 20 000) bound NAD^+ (PEG–NAD^+), shown in Figure 5. Table II shows the factors for the peak current enhancements for three different concentration ratios of NAD^+ with **1** and **12**, respectively (1:1, 1:2, 1:5). In the case

Table II. Factors for the Cathodic Peak Current Enhancements for Complexes 1 and 12 (5×10^{-4} M) in the Presence of NAD^+ at a Glassy Carbon Cathode in 0.1 M Tris/HCl Buffer (pH 7.5)

	[1]:[NAD^+]			[12]:[NAD^+]		
υ, mV/s	1:1	1:2[a]	1:5[a]	1:1	1:2[a]	1:5[a]
9	2.00	2.73	5.18	1.88	2.98	5.66
25	2.08	2.74	4.92	1.94	2.94	5.15
49	1.98	2.65		2.04	3.05	4.78
81	1.95	2.55		1.97	2.82	4.32
121	1.88	2.41		2.05	2.65	
169	1.81	2.22		1.98	2.61	
225	1.79					
289	1.74					
361	1.71					
441	1.63					
529	1.60					
625	1.59					
729	1.51					

[a] At higher scan rates and higher NAD^+ concentrations adsorption effects do not allow the determination of the exact peak currents.

of **12** the maximum values of 2, 3, and 6, respectively, are almost reached at scan rates of 9 $mV \cdot s^{-1}$, indicating a very fast homogeneous redox reaction between the rhodium hydride complex $[(C_5Me_5)RhH(4\text{-}Mebpy)]^+$ and NAD^+. The same is true for complex **1**, however to a somewhat smaller extent.

Because the catalytic activity toward the high molecular weight cofactor (PEG–NAD^+) as well as for $NADP^+$ is practically as high as for NAD^+ itself, the rhodium complexes studied are good mediators for the electrochemical regeneration not only of NADH but also of NADPH and PEG–NADH, allowing the performance of electroenzymatic reactions with a multitude of enzymes. In a flow-through membrane reactor, the necessary use of high molecular weight cofactors like **11** does not seem to impose any complications.[10] The good catalytic activity of **11** is demonstrated in Figure 3.

Plotting the reductive peak currents of the rhodium complexes in the presence of equimolar amounts of NAD^+ versus the square root of the scan rates yields a linear relationship with a slope twice as high as in the absence of NAD^+ for active complexes at slow scan rates. The overall rate is thus determined by the heterogeneous electron transfer only. According to the different activities of the complexes, a deviation from a straight line can be observed at higher scan rates because the time for the regeneration step is diminished. In this case the coupled homogeneous chemical reaction becomes rate determining. Figure 6 shows a typical example for a $i_{p,red}$ vs $\sqrt{\upsilon}$ plot at different pH values. At pH 3.7 and 7 the peak current vs $\sqrt{\upsilon}$ relation in the presence of NAD^+ is linear up to 729 $mV \cdot s^{-1}$. At pH 9, however, the slope of the curve is decreasing for higher scan rates. This indicates that the heterogeneous electron transfer is no longer rate determining. The rate-determining step, instead, is now the formation of the hydride complex, as already indicated by the reversible cyclic voltammogram at pH 9 and 10 in Figure 1 in the absence of NAD^+. The catalytic cycle can thus be represented by eqs 1–5 (see above) and eq 8.

$$[(C_5Me_5)Rh^{III}H(bpy)]^+ + L + NAD(P)^+ \rightarrow [(C_5Me_5)Rh^{III}(bpy)L]^{2+} + NAD(P)H \quad (8)$$

From Figure 7 the relative catalytic activities of complexes 1–5 and 8–10 toward $NAD(P)^+$ can be deduced. For complexes **8** and **9** (L′ = bpy-5-OH, bpy-5-OAc) the i_p vs $\sqrt{\upsilon}$ plots in the presence of NAD^+ are linear up to relatively high scan rates. They have the highest catalytic activity of all the complexes studied. In the case of complexes **1–3**, **5**, **10**, and **12** (L′ = bpy, phen, 4,4′-Me_2bpy, bpy-4,4′-$(COOH)_2$, bpy-5-CH_2OEt, 4-Mebpy) the slopes are decreasing at higher scan rates, however with complex **12** only to a very small extent (Table II). Complex **4**, however, shows almost no peak current increase at high scan rates, thus it has the lowest activity of the complexes mentioned up to now. Complexes **6** and **7** (L′ = bpy-4,4′-(COOEt), bpy-5,5′-$(COOEt)_2$) show no peak current increase in the presence of NAD^+ even at slow scan rates. This was proven for **7** in a controlled-potential electrolysis in the presence of NAD^+ at pH 7.5. Only traces of NADH were formed after 3 h. Thus, the order of the electrocatalytic activity of the complexes toward NAD^+ reduction is $8 \approx 9 > 3 \approx 12 > 1 > 2 \approx 5 \approx 10 > 4 \gg 6 \approx 7$. This order mainly reflects the basicity of the nitrogen-containing ligand, which influences the electron density at the rhodium central atom. Higher electron density at the rhodium leads to a faster formation of the hydride complex. This points to the fact that, in the indirect electrochemical NAD^+ reduction, the formation of the rhodium hydride complex is the rate-determining step. The same is true in the formate-driven redox catalytic reduction of NAD^+ using these rhodium complexes as catalysts, in which the electrode is replaced by formate as the reducing agent (see below). For complex **13** the catalytic activity could not be determined because its reduction potential is so negative that it interferes with the direct reduction of NAD^+. For the iridium complex **14** no catalytic activity toward NAD^+ was observed.

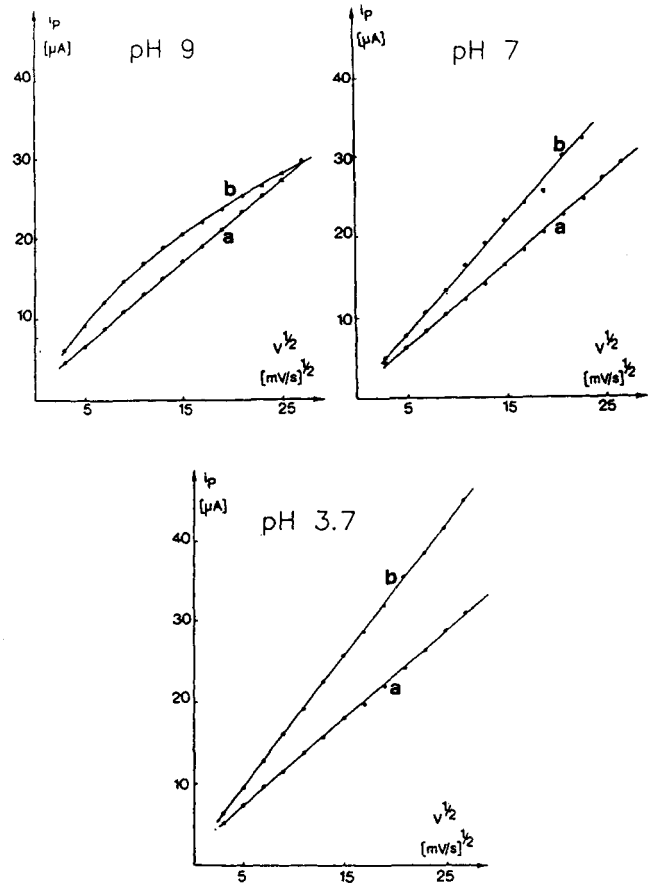

Figure 6. Plot of cathodic peak currents versus the square roots of the scan rates from the cyclic voltammograms of complex **3** (5×10^{-4} M) in the absence (a) and presence (b) of NAD^+ (5×10^{-4} M) in 0.1 Tris/HCl buffer at a glassy carbon cathode under pH variation (no background current correction).

UV Spectroscopic Study of the Rhodium(III) Complex Catalyzed Reaction between $NAD(P)^+$ and For-

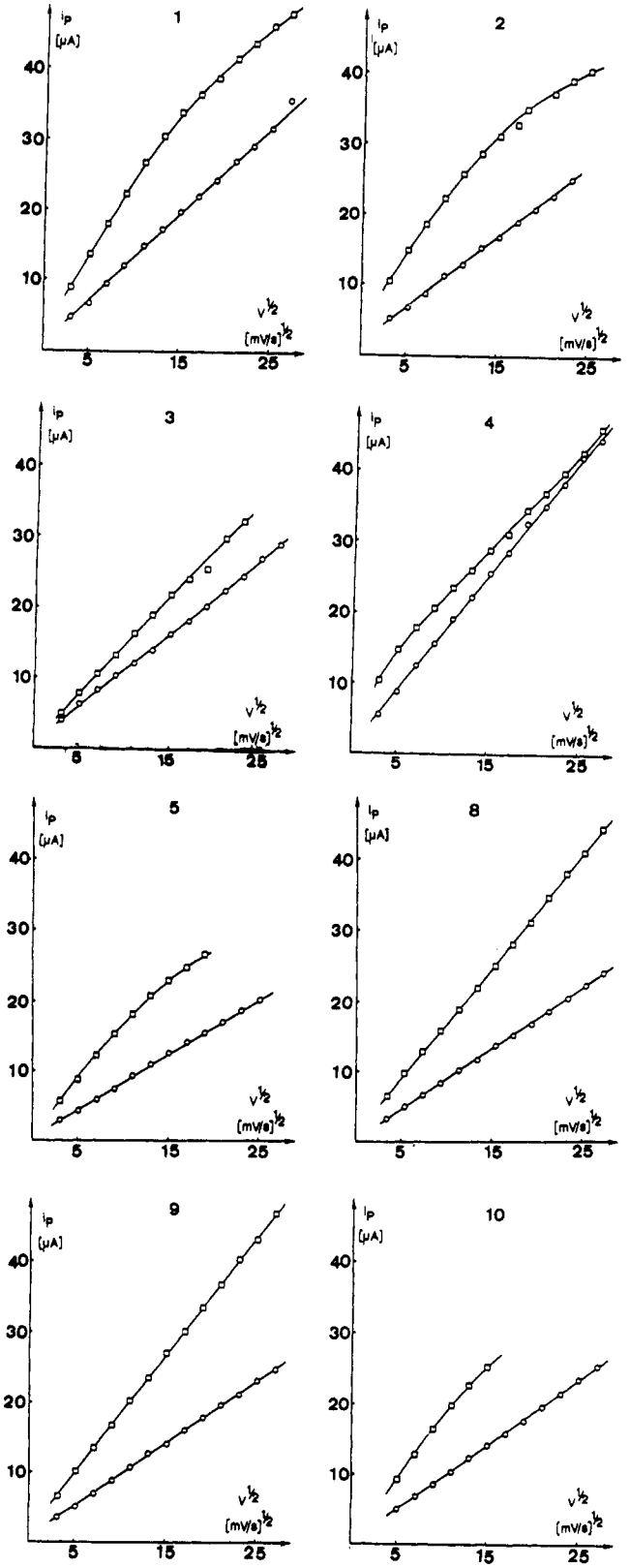

Figure 7. Plot of cathodic peak currents versus the square roots of the scan rates from the cyclic voltammograms of complexes **1–5** and **8–10** (5×10^{-4} M) in absence (○) and presence (□) of NAD^+ (5×10^{-4} M) in 0.1 Tris/HCl buffer at a glassy carbon cathode.

mate. In a preliminary communication, we have already shown that complexes **1**, **3**, and **4** are effective catalysts for the chemical reduction of $NAD(P)^+$ using formate as donor.[9] The catalytic activities of the different complexes in this reaction can be compared and kinetic parameters

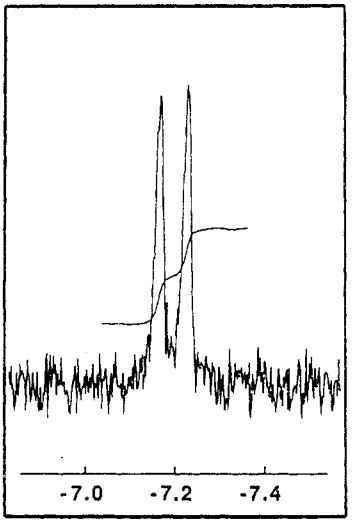

Figure 8. ^1H NMR signal for the rhodium hydride complex of compound **4** (10^{-2} M) measured in D_2O/HCOONa at pH 8.5 (set by addition of NaOD) under argon atmosphere; ratio of **4** to $HCOO^-$ about 1:10.

may be obtained, if the time dependence of the NAD(P)H formation is followed at 340 nm by UV spectroscopy. The turnover frequency (TF), that is the number of regenerative cycles of the rhodium catalysts per hour, can thus be calculated. The following values for the reduction of NAD^+ (3.8×10^{-4} M) by sodium formate (0.5 M) in sodium phosphate buffer (0.1 M) at pH 7.0 at 38 °C were obtained for the different complexes (2.5×10^{-5} M): **1**, TF = 77.5; **2**, TF = 70.9; **3**, TF = 76.4; **4**, TF = 60.9; **5**, TF = 72.4; **8**, TF = 74.1; **9**, TF = 70.9; **10**, TF = 67.5; **11** (PEG-bound complex), TF = 43.3 (all values in h^{-1}). Of the complexes studied, **1** shows the fastest overall reaction rate while **4** is very slow. This is in accordance with the cyclic voltammetric measurements, indicating a slowing down of the hydride complex formation by steric interference of the 6,6′-methyl groups. Very interesting was the fact that the polyethylene glycol (MW 20000) bound complex **11** shows an appreciable turnover frequency. In all of these cases a linear increase of the NADH concentration up to quantitative NAD^+ turnover was observed. Therefore the reaction is zero order in NAD^+. By variation of the formate concentration, Michaelis type kinetic behavior is observed, indicating a preequilibrium, with formation of a complex between Rh^{III} and formate, is the initial step.[9] A K_M value of 140 mM was determined for complex **1**. The subsequent step of the reaction must be formation of the rhodium(III) hydride with extrusion of CO_2. This is probably the rate-determining step of the overall reaction. The pronounced isotopic effect observed, when DCO_2D was used instead of HCO_2H, supports this hypothesis, while use of D_2O instead of H_2O had almost no influence on the overall reaction rate.[9] The follow-up hydride transfer to NAD^+ must be very fast. The following mechanism can thus be deduced:

$$[(C_5Me_5)Rh^{III}(bpy)L]^{2+} + HCO_2^- \rightleftharpoons [(C_5Me_5)Rh^{III}(bpy)(HCO_2)]^+ + L \quad (9)$$

$$[(C_5Me_5)Rh^{III}(bpy)(HCO_2)]^+ \rightarrow [(C_5Me_5)Rh^{III}H(bpy)]^+ + CO_2 \quad (10)$$

$$[(C_5Me_5)Rh^{III}H(bpy)]^+ + L + NAD(P)^+ \rightarrow [(C_5Me_5)Rh^{III}(bpy)L]^{2+} + NAD(P)H \quad (8)$$

The existence of the intermediate rhodium hydride complex could be established in the case of compound **4** by ^1H NMR analysis at pH 8.5 in D_2O/HCOONa. A

Table III. Turnover Frequencies (h^{-1}) of Complexes 10 and 11 for the Catalysis of the Reduction of NAD^+, $NADP^+$, and PEG-NAD^+ by Formate[a]

	NAD^+		$NADP^+$		PEG-NAD^+	
temp, °C	10	11	10	11	10	11
25	20.3	13.3	20.7	12.3	16.6	9.9
38	67.5	43.3	67.5	39.5	56.4	31.8

[a] 0.5 M HCOONa, 3.8×10^{-4} M cofactor, 2.5×10^{-5} M 10 or 11 in 0.1 M sodium phosphate buffer (pH 7.0) under an argon atmosphere.

doublet at −7.2 ppm clearly indicates the hydride ligand (Figure 8).

With complexes 6 and 7 the NADH formation slows down very much with time, indicating that in these cases hydride transfer is the rate-determining step. 13 and 14 behave similarly.

In the case of complex 10, we studied the influence of the buffer system (sodium phosphate or Tris/HCl) and the formate counterion (sodium or ammonium) on the turnover frequency. With sodium phosphate buffer the pH optimum for the reduction of NAD^+ by sodium formate is obtained at pH 8 due to increasing hydrogen formation at lower pH values. At higher pH the labile aquo ligand is replaced by the stronger coordinated hydroxy ligand, slowing down the ligand exchange by formate (eq 9). In the presence of ammonium formate as the reducing agent the pH optimum is found at pH 6. Under more basic conditions the free ammonia seems to act as a monodentate ligand for the rhodium central atom, which is more difficult to exchange by formate (eq 9). Tris/HCl buffer slows down the NADH formation drastically. This may also be explained by the action of Tris as a strong ligand to rhodium, making the starting complex more stable.

In the case of complexes 10 and 11 it could also be shown that not only NAD^+, but also $NADP^+$ and PEG–NAD^+ (PEG MW 20 000) can be reduced catalytically by sodium formate (Table III). The turnover frequency of 10 is identical for NAD^+ and $NADP^+$ and about 20% lower for the high molecular weight cofactor PEG–NAD^+. 11 behaves very similarly; however, because of the binding to PEG the turnover frequencies are between 30 and 40% lower. The reaction rate in the presence of 11 is also independent of the NAD^+ concentration. The activation energies for the reduction of NAD^+ and PEG–NAD^+ catalyzed by 10 ($E_A(NAD^+)$ = 16.3 kcal·mol^{-1}, E_A(PEG–NAD^+) = 16.4 kcal·mol^{-1}) and 11 ($E_A(NAD^+)$ = 15.3 kcal·mol^{-1}, E_A(PEG–NAD^+) = 16.8 kcal·mol^{-1}) were determined by rate measurements at different temperatures (17.3, 25.7, 32.1, 40.0 °C). The increase of the molecular weight of the cofactor as well as of the complex does not influence the activation energy. This is important for the application of 11 as a catalyst for the chemical cofactor regeneration for enzymatic reactions in a flow-through membrane reactor.[10]

Acknowledgment. We thank Mr. Mouchel, University Lille, for technical NMR assistance. We thank the Fonds der Chemischen Industrie and the BASF Aktiengesellschaft for financial support and the Fonds der Chemischen Industrie (S.H.) and the Alexander-von-Humboldt-Stiftung (R.R.) for fellowships. The gift of chemicals by Degussa AG is gratefully acknowledged.

Ring Migration Reactions of $(C_5Me_5)Rh(PMe_3)H_2$. Evidence for η^3 Slippage and Metal-to-Ring Hydride Migration

William D. Jones,* Valerie L. Kuykendall, and Anthony D. Selmeczy

Department of Chemistry, University of Rochester, Rochester, New York 14627

Received July 17, 1990

The reactions of $(C_5Me_5)Rh(PR_3)H_2$ (PR_3 = PMe_3, PMe_2Ph, $PMePh_2$, PPh_3) with D_2 gas occur quickly at 25 °C, leading to the stepwise exchange of hydrogen for deuterium. Kinetic studies indicate a second-order reaction mechanism involving rhodium and deuterium. $(C_5Me_5)Rh(PMe_3)H_2$ also reacts with PMe_3 at 40 °C to give C_5Me_5H and $HRh(PMe_3)_4$, a reaction that also displays bimolecular kinetics. Isotope effect studies show no rate difference with the dideuteride rhodium complex. The mechanism(s) of these reactions are discussed in light of the kinetic requirements. The reactions of $(C_5Me_5)Rh(PR_3)(Ph)H$ with H_2 have also been studied and found to lead to $(C_5Me_5)Rh(PR_3)H_2$.

Introduction

Reactions of metal cyclopentadienyl complexes and their methylated derivatives have been the subject of intense study over the past few decades. While in many cases this ligand has been present as a spectator for much of the chemistry that occurs at either the metal center or a coordinated ligand, there is also good evidence for noninnocent involvement of this η^5 ligand. In particular, the importance of $\eta^5 \rightarrow \eta^3$ ring slippage[1] and metal-to-ring migration reactions[2] have both been cited in recent literature.

Complexes of the general formula $(C_5R_5)M(L)(R)H$ and $(C_5R_5)ML_2$ (M = Rh, Ir; R = H, Me; L = PMe_3, CO, C_2H_4) have been found to be generally very active for the activation of C–H bonds.[3] While most evidence points toward

(1) O'Connor, J. M.; Casey, C. P. *Chem. Rev.* **1987**, *87*, 307–318 and references therein. Rerek, M. E.; Basolo, F. *Organometallics* **1983**, *2*, 372–376. Schuster-Woldan, H. G.; Basolo, F. *J. Am. Chem. Soc.* **1966**, *88*, 1657–1663. Cramer, R. E.; Seiwell, L. P. *J. Organomet. Chem.* **1975**, *92*, 245–252.

(2) Benfield, F. W. S.; Green, M. L. H. *J. Chem. Soc., Dalton Trans.* **1974**, 1324–1331. Crabtree, R. H.; Dion, R. P.; Gibboni, D. J.; McGrath D. V.; Holt, E. M. *J. Am. Chem. Soc.* **1986**, *108*, 7222–7227. Green, M. L. H. *Pure Appl. Chem.* **1978**, *50*, 27–35. Jones, W. D.; Maguire, J. A. *Organometallics* **1985**, *4*, 951–953. Fachinetti, G.; Floriani, C. *J. Chem. Soc., Chem. Commun.* **1974**, 516–517. Benfield, F. W. S.; Green, M. L. H. *J. Chem. Soc., Dalton Trans.* **1974**, 1324–1331. Werner, H.; Hofmann, W. *Angew. Chem., Int. Ed. Engl.* **1977**, *16*, 794–795.

0276-7333/91/2310-1577$02.50/0